AD-A033 713 GTE LABS INC WALTHAM MASS F/G 9/5
HERTZIAN ARRAY SWITCH INVESTIGATION.(U)
OCT 76 J M PROUD, D H BAIRD, W H MCNEILL F30602-75-C-0164
UNCLASSIFIED RADC-TR-76-301 NL

1 OF 1
AD
A033713

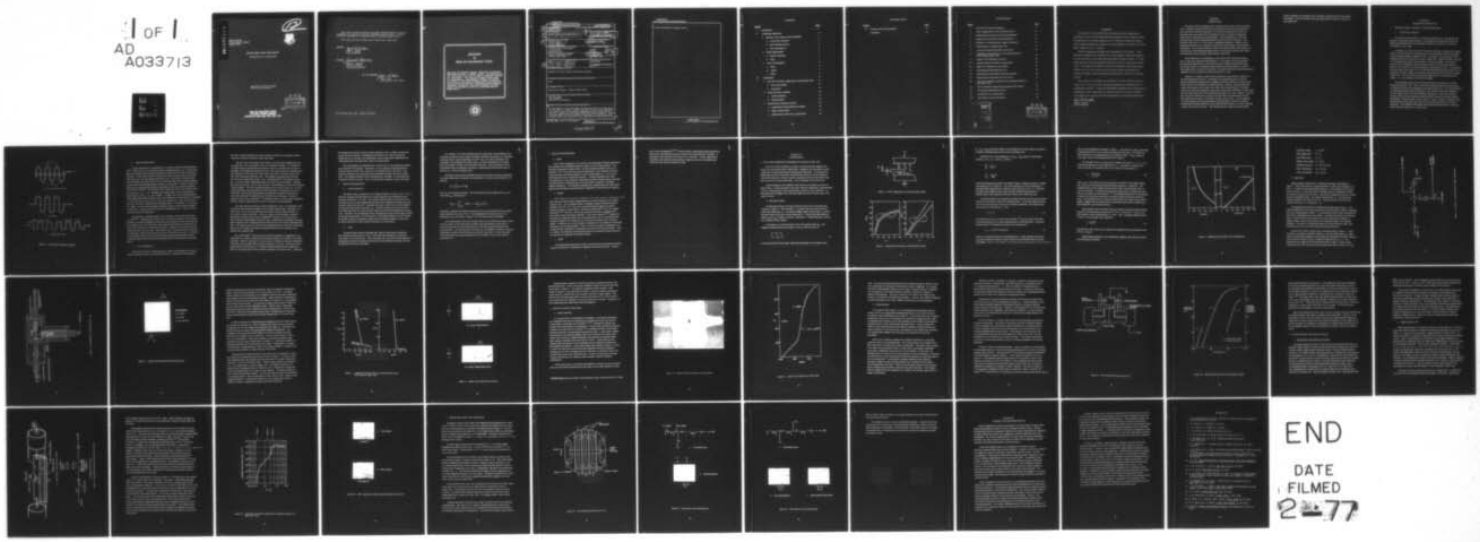

END
DATE
FILMED
2-77

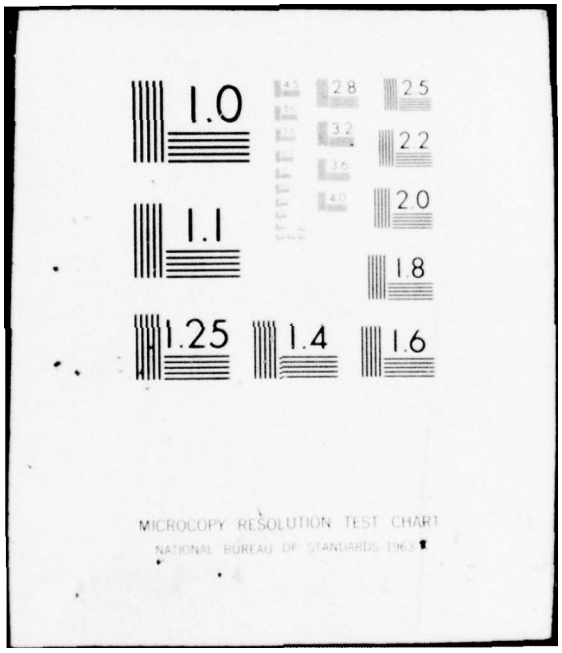
1.0
1.1
1.25
1.4
1.6
2.8
2.5
3.2
2.2
3.6
2.0
4.0
1.8
MICROCOPY RESOLUTION TEST CHART
NATIONAL BUREAU OF STANDARDS 1963

12 B.S.

RADC-TR-76-301
Final Technical Report
October 1976

HERTZIAN ARRAY SWITCH INVESTIGATION

GTE Laboratories Incorporated

ROME AIR DEVELOPMENT CENTER
AIR FORCE SYSTEMS COMMAND
GRIFFISS AIR FORCE BASE, NEW YORK 13441

This report has been reviewed by the RADC Information Office (OI) and is releasable to the National Technical Information Service (NTIS). At NTIS it will be releasable to the general public including foreign nations.

This report has been reviewed and is approved for publication.

APPROVED: Frank E Welker

FRANK E. WELKER
Project Engineer

APPROVED: Joseph J Ryerson

JOSEPH L. RYERSON
Technical Director
Surveillance Division

FOR THE COMMANDER: John P. Huss

JOHN P. HUSS
Acting Chief, Plans Office

Do not return this copy. Retain or destroy.

MISSION
of
Rome Air Development Center

RADC plans and conducts research, exploratory and advanced development programs in command, control, and communications (C^3) activities, and in the C^3 areas of information sciences and intelligence. The principal technical mission areas are communications, electromagnetic guidance and control, surveillance of ground and aerospace objects, intelligence data collection and handling, information system technology, ionospheric propagation, solid state sciences, microwave physics and electronic reliability, maintainability and compatibility.

UNCLASSIFIED

SECURITY CLASSIFICATION OF THIS PAGE (When Data Entered)

REPORT DOCUMENTATION PAGE

READ INSTRUCTIONS BEFORE COMPLETING FORM

1. REPORT NUMBER: RADC-TR-76-301	2. GOVT ACCESSION NO.
3. RECIPIENT'S CATALOG NUMBER	
4. TITLE (and Subtitle): HERTZIAN ARRAY SWITCH INVESTIGATION •	5. TYPE OF REPORT & PERIOD COVERED: Final Technical Report. 18 June 1975 — 18 June 1976
6. PERFORMING ORG. REPORT NUMBER: N/A	
7. AUTHOR(s): Joseph M. Proud, Donald H. Baird, William H. McNeill	8. CONTRACT OR GRANT NUMBER(s): F30602-75-C-0164
9. PERFORMING ORGANIZATION NAME AND ADDRESS: GTE Laboratories Incorporated, 40 Sylvan Road, Waltham MA 02154	10. PROGRAM ELEMENT, PROJECT, TASK AREA & WORK UNIT NUMBERS: 62702F, 55730205
11. CONTROLLING OFFICE NAME AND ADDRESS: Rome Air Development Center, Griffiss AFB NY 13441	12. REPORT DATE: October 1976
	13. NUMBER OF PAGES: 54
14. MONITORING AGENCY NAME & ADDRESS (if different from Controlling Office): Same	15. SECURITY CLASS. (of this report): UNCLASSIFIED
16. 5573	15a. DECLASSIFICATION/DOWNGRADING SCHEDULE: N/A
17. 02	

16. DISTRIBUTION STATEMENT (of this Report)

Approved for public release; distribution unlimited.

17. DISTRIBUTION STATEMENT (of the abstract entered in Block 20, if different from Report)

Same

18. SUPPLEMENTARY NOTES

RADC Project Engineer: Frank E. Welker (OCTP)

19. KEY WORDS (Continue on reverse side if necessary and identify by block number)

Hertzian Arrays
Fast Triggering
Optoelectronic Triggering

20. ABSTRACT (Continue on reverse side if necessary and identify by block number)

An investigation of fast, high power switching with jitter in the sub-nanosecond time domain is reported. Methods involving field distortion triggering in high pressure gases, photoconduction triggering in aprotic liquids and optoelectronic triggering in solid semiconductors have been investigated. The most promising avenue for further research is identified in the latter area where extremely small jitter and rapid turn-on capabilities are well matched to the →

DD FORM 1 JAN 73 1473 EDITION OF 1 NOV 65 IS OBSOLETE

UNCLASSIFIED

SECURITY CLASSIFICATION OF THIS PAGE (When Data Entered)

406462

timing requirements in Hertzian arrays.

CONTENTS

CONTENTS CONT'D

ILLUSTRATIONS

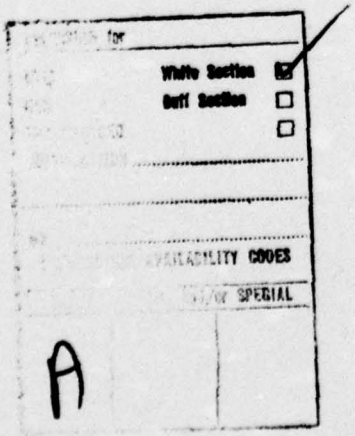

EVALUATION

The objective of this effort was to develop precision timing switch techniques for use in multi-switch Hertzian generators and in Hertzian arrays. The application of Hertzian generators as r-f sources in radar and communication systems depends very strongly on the development of switches with jitter small compared to one r-f period.

Several triggering techniques were investigated in the effort. Field distortion triggering was evaluated over a wide range of operating parameters but was limited by a relatively high percentage of missed closures. UV triggered spark gap switches performed well but are limited to applications below 1 GHz. Photoconduction induced in silicon by microjoule laser pulses demonstrated very fast rise time and very low jitter giving the potential for microwave frequency Hertzian generator operation but is limited in operating voltage.

The results of this effort are considered to be very useful in that the limitations on very low jitter switching techniques were specified and experimentally verified. In addition preliminary experiments with optoelectronic triggering in solid semiconductors indicate promise of giving the required low trigger jitter required for Hertzian generators at microwave frequencies.

Frank E. Welker

FRANK E. WELKER
Project Engineer

SECTION I
INTRODUCTION

The object of this investigation was to identify means for the low jitter initiation of fast, repetitively operated switches with performance parameters appropriate for use in microwave Hertzian transmitters. Of particular interest in this context are Hertzian devices involving arrays of switches in series or parallel arrangements which require a high degree of synchronization. The investigation was concerned primarily with one such configuration known as the Frozen Wave Generator. The potential of this device as a very simple, lightweight transmitter, capable of multi-megawatt performance, is of interest for both radar and electronic countermeasures applications. The specific performance goals of the switch sought in this program are commensurate with multimegawatt generation of microwaves by means of the Frozen Wave Generator in the frequency range between 1 and 10 GHz.

Known methods for accomplishing, at least some of the switch performance goals, suffer from complexity and inefficiency. For example, it has been shown[1] that ultraviolet light pulses can provide the necessary switch synchronization when the switch is placed in a momentary (nanoseconds) overvoltage condition. However, when applied to the Frozen Wave Generator, the pulsed overvoltage requirement becomes untenable in devices designed to operate much above 0.5 GHz.

Initially, we sought to trigger rapid breakdown in liquid dielectric switches via fast photoconduction processes. Conceptually, the approach has many attractive features including the high dielectric strength and chemical stability of certain aprotic liquids which are also thought to be photoconducting. However, the photoconducting response was found to be too small to be useful, and we turned instead, to impulse-driven, field distortion triggering in high pressure gases where initiation of transmission line spark gaps with jitter in the sub-nanosecond range was, in fact, achieved. However, this success was offset by the statistical characteristics of missed switch closures which degrade performance, particularly in large, series arrays. The investigation of a third technique involving quasimetallic photoconduction in silicon successfully demonstrated switching with jitter in the picosecond time domain in an array composing a small Frozen Wave Generator. This technique seems to offer an approach which

could be extended to much higher power and higher frequencies than in the present investigation. Such an extension could open important new avenues for microwave pulse generation.

SECTION II
TECHNOLOGY BACKGROUND

1. HERTZIAN ARRAY CONTEXT OF THE INVESTIGATION

a. Frozen Wave Generator

The Frozen Wave Generator is a simple and potentially very efficient Hertzian generator employing multiple switches. Its principles of operation and various configuration possibilities have been thoroughly considered in Reference 1 and will be reviewed here very briefly.

A schematic of a basic six-cycle Frozen Wave Generator is illustrated in Figure 1. In this case six elements of a transmission line which can support TEM mode propagation are initially charged to potentials + and - V_0 as shown. The result under static conditions is then the "frozen wave" shown in Figure 1(b). When the switches A through G are simultaneously closed, the frozen wave is free to propagate. Two identical square waves of amplitude V_0 (peak-to-peak) will appear, one leaving the system at Switch A, the forward wave, and one at Switch G, the regressive wave. A transmission line short placed just beyond G reverses the latter which then joins the forward wave as illustrated, thereby creating a pulse having a width equal to twice the electrical length of the device. The wave period will equal two transit times of each segment of the system, i.e., the segments are one-half wavelength.

The particularly attractive feature of the Frozen Wave Generator is its high theoretical efficiency, 80%. That is, 80% of the energy initially stored in the system is released in the sine wave component of the output square wave. One of the difficulties in achieving this high conversion efficiency is that associated with the simultaneous and fast rising closure of all of the switches of the system. Jitter in the initiation process produces random frequency modulation which robs spectral energy from the fundamental. If jitter includes "missed closures," that is, lag time variations exceeding one-half RF period, the device may not in fact produce an output, or at least a useful one. The probability of the latter event increases with the number of switches which must act in concert for a useful output.

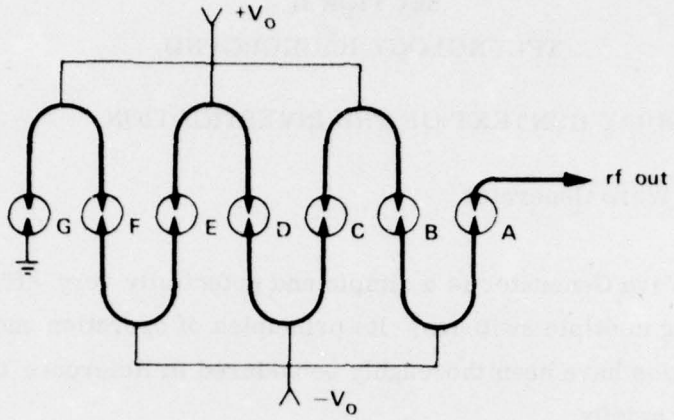

(a) Six Cycle Frozen Wave Generator

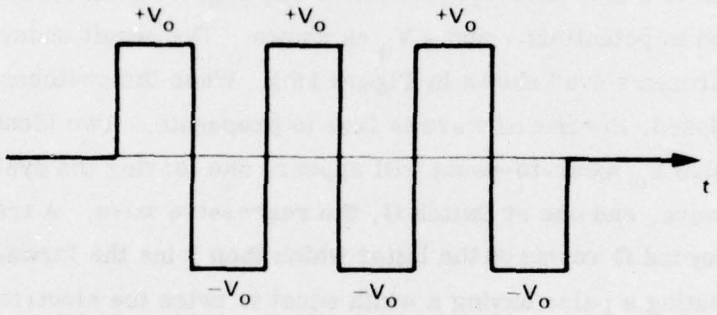

(b) Frozen Wave

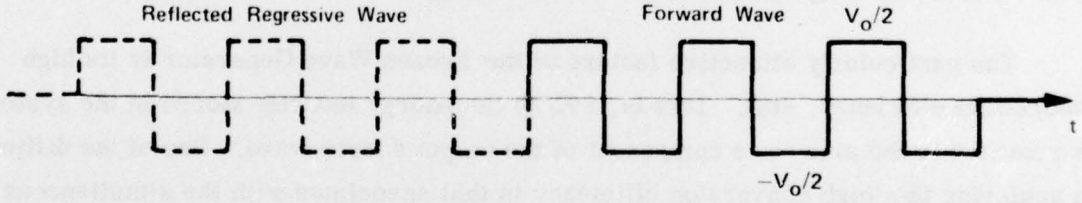

(c) Travelling Wave Output

Figure 1. Frozen Wave Generator Schematic

b. Other Hertzian Devices

A single switch device is exemplified by a resonant cavity-type Hertzian generator[2]. Such sources are of particular interest at high frequency (e.g., 10 GHz) where physical constraints militate against multiswitch structures such as the Frozen Wave Generator. If the relative phase of large arrays of these sources could be accurately controlled, some very interesting possibilities arise. One of these would be in the area of synthetic apertures where one could achieve the high range resolution inherent in short pulses with the high angular resolution of the aperture. Another example lies in the area of electronically steerable arrays where rapid scan and small resolution cells could be achieved. Such systems would ordinarily involve large numbers of individual sources, e.g., $\sim 10^3$, although special applications can be visualized which would require as few as, say, ten elements. In either case, and in contradistinction to the multiswitch Hertzian example above, the elements to be synchronized or controlled in a phased array are electrically in a parallel configuration. Thus, the statistics of jitter may have quite a different impact on performance. For example, the misfiring of a single, or even several elements contributes in only a small way to the output of a large array. On the other hand, in the series multiswitch case, a single misfiring can even preclude an output pulse.

The Travatron is another Hertzian device which has seen considerable initial success[3,4,5]. Schematically similar to the Frozen Wave Generator, the Travatron switches are closed sequentially as they become overvolted by an input traveling wave. In its simplest form, the Travatron is theoretically 40% efficient as compared to the ideal value of 80% for the Frozen Wave Generator. However, the relative simplicity of the Travatron is its key asset. Switch jitter in the Travatron can lead to spectrum spreading and a degree of fm noise just as in the Frozen Wave Generator. The ability to command the switch closures in the appropriate timing sequence with low jitter could reduce these effects and elevate the signal quality of this potentially important device.

c. Prior Switching Art

The spark gap switch, employing gaseous, liquid or solid dielectric, has been used in virtually all of the reported Hertzian devices. In the present investigation,

the scope of switch candidates has been expanded to include an investigation of photo-conduction controlled switching in liquids and solids.

The spark gap is well known for its ability to provide rapid switching between a very high and a very low impedance state via avalanche breakdown. It is suitable for very high voltage (multikilovolt) operation and, therefore, provides the capacity for switching in very high power Hertzian devices. The central problem in applying spark gap technology to devices like the Frozen Wave Generator or the other arrays cited above lies in the jitter which may exist. The problems associated with spark gap jitter have been extensively studied. In an in-depth study[6] of the triggered spark gap, as many as fifteen triggering methods were cited from the literature. Although this study surveyed the art up to 1965, the more recent literature reveals only variations of these methods. The most promising techniques for low jitter seem to be: (1) ultra-violet illumination of the electrodes of a spark gap which is momentarily in an over-volted state, (2) field distortion methods involving three electrode systems, and (3) laser pulse initiation of breakdown in the dielectric space of the gap. The latter technique seems to be a useful one[7], but typically involves a laser of more complexity than the relatively simple Hertzian devices of interest in this investigation.

One of the attractive features of optical triggering, such as UV triggering, is the isolation afforded between the trigger source and the triggered gap. Since this is an optical path, one is not concerned with such problems as high voltage isolation or capacitance of control electrodes. Moreover, the low jitter capability of pulsed UV illuminated overvolted gaps has been established[8] and may be as small as 25 ps. These referenced experiments involved the rapid, simultaneous overvolting of two gaps with provision for the UV light produced by the discharge of one switch to illuminate the other. The effective spectral content of the triggering pulse was observed to be between 200-300 nm, the trigger mechanism being photo-induced electron emission at the cathode of the triggered gap.

In a recent study[1], some success was found in applying UV triggering of over-volted gaps as a means to synchronize the multiple switches of a 250 MHz Frozen Wave Generator. However, the degree of success became marginal at generator frequencies of 500 MHz and the method became totally unworkable at 1.3 GHz. The failure of this method stems from the need for overvoltage conditions which must be brought about with ever increasing speed as the microwave frequency of the device rises. Ultimately

the charging time and the microwave period converge so that, in effect, the spectrum energy conversion process, fundamental to Hertzian devices, fails to take place. Beyond this basic limitation, the methodology creates considerable complexity in the efficient generation and application of high overvoltage pulses.

This investigation was undertaken with a specific aim of overcoming the problems associated with UV triggering. Specifically, we have explored switching methods in which the initial electric field is below the self breakdown field of the switch. This condition eliminates from consideration those methods requiring a pulsed overvolted state. The candidate methods of this investigation have included: (1) photoconduction switching in liquids and solids, and (2) field distortion triggering in gases and liquids.

2. SWITCH REQUIREMENTS

a. General Objectives

The goals of this investigation are for triggered switch techniques which could be utilized in multigap Hertzian generators to yield megawatt level performance in the frequency range from 1 to 10 GHz. The specific numerical goals of the program were formulated in terms of the fundamental properties of the triggered spark gap switch and included voltage hold-off (60 kV), impedance (50 ohms), jitter (50 ps), pulse repetition rate (400 pps) and risetime (less than 1 ns). With the exception of the goal for jitter, all of these objectives have been achieved routinely in prior Hertzian generator development. Therefore, the concentration of this investigation has dealt with the jitter problem. In seeking new approaches not involving pulse overvoltage conditions, we have relaxed the specific voltage and impedance targets to admit switching methods in media such as silicon where lower values of these parameters are more natural.

b. Jitter

The goals of this program regarding jitter allow for the practical realization that two given switches may not, in fact, close with 100% reliability over their lifetime within a 50 ps time interval. Some misfirings may be tolerated in these objectives although the tolerance will depend upon the nature of the particular Hertzian array and the statistical character of the jitter.

For example, if P is the probability that one switch fails to close within the prescribed 50 ps interval, then a system containing n switches will produce an "acceptable" waveform with an overall probability of $(1-P)^n$. Thus, if a typical switch has a 5% probability of exceeding the 50 ps jitter limit, a waveform produced by a 20-switch device will exhibit a "faulty" cycle about 65% of the time. The seriousness of such a fault depends upon its magnitude, the degree of signal quality desired and the type of device (e.g., series or parallel array).

The shape of the lag time distribution about its mean value can also be important. If a normal distribution is assumed, the probability of a switch closure with delay t is given by:

$$P(t) = \sqrt{\frac{2}{\pi}} \exp - t^2/2t_0^2$$

where t_0 is the standard deviation. The probability that the lag might exceed a particular value t_m is then given by:

$$P(t_m) = \int_{t_m/t_0}^{\infty} P(t)dt = 1 - \mathrm{erf}\left(t_m/\sqrt{2}\, t_0\right)$$

If the jitter, equated to the standard deviation is 50 ps, the probability that excursions greater than this will occur is 0.32. The probability that excursion as great as a half-period occur, say 500 ps, is only 6×10^{-5} for this assumed distribution.

Actual distributions with rms deviations close to 50 ps showed excursions as large as 500 ps about 2 to 3% of the time according to the measurements of Reference 1. This is because the measured distribution was unlike the normal distribution in the outer extremes. An actual generator built with, say, 20 switches, having the measured distribution, would have this serious flaw about 50% of the time. For the same jitter but one described by a normal distribution, the occurrence of such a flaw would be extremely rare.

3. AREAS OF INVESTIGATION

a. Gases

Prior to this investigation, the majority of developments in Hertzian generators have exploited the outstanding properties of gases as the switching medium. The particular advantages of gases include: the high breakdown strength which can be achieved ($> 10^6$ V/cm); the direct pressure dependence of this strength; the variety, simple chemistry and wide temperature range of useful gases (e.g., air); and the self-healing and ease of replacement features. Partially offsetting these useful characteristics are the sometimes complicating mechanical design aspects associated with high pressure containment and, as we have noted, limitations in available trigger mechanisms. The present investigation has considered gaseous media spark gaps and has attempted to extend the known capabilities of field distortion triggering.

b. Liquids

Liquid dielectric switches, employed by the early Hertzian researchers circa 1900, have been unsuccessful in applications such as those visualized in the modern Hertzian array. The dc voltage breakdown strength of typical insulating liquids is relatively low (10^4 to 10^5 V/cm) and is characteristically weakened by gaseous products produced by vaporization or chemical decomposition[9] and by the bridging of particles.[10] Moreover, serious decomposition and further degradation take place under repetitive sparking conditions. Some recent research,[11] dealing with electronically conducting liquids, has demonstrated that electron multiplication and repetitive millijoule-level sparking can be observed in purified aprotic molecular liquids. In addition some of these liquids are thought to be semiconductors possessing properties such as photoconduction. Thus, one aim of the present investigation was to determine the possibilities of exploiting some of these new-found properties. Thus, one might at once eliminate pressurization problems associated with gases and open new avenues for triggering the switching medium.

c. Solids

Semiconducting junction devices which can switch in the sub-nanosecond domain, cannot be considered for application in megawatt level Hertzian devices. However,

some recent investigations[12, 13] of laser induced, quasimetallic photoconduction in silicon have demonstrated picosecond risetime and picosecond jitter switching. It also appears that megawatt level devices may be possible. We have explored this technology in the present program taking an approach which is aimed specifically at the use of the method in Hertzian Arrays.

SECTION III
INVESTIGATION

1. FAST FIELD DISTORTION TRIGGERING IN GASEOUS SPARK GAPS

The use of a third electrode to produce local field distortion leading to the closure of a spark gap switch is widely known, although to our knowledge no switch of this type has approached the performance goals cited above. In most previous applications of the three electrode, field distortion switch the system impedance, switch self-inductance, and inter-electrode capacitance have all contributed to lag and rise times of several nanoseconds. Jitter is typically of this same order.

Taking advantage of the relatively small energy to be handled in the case of interest here, we have attempted to limit inter-electrode capacitance to approximately 2 pF in a switch geometry which approximates a uniform 50 ohm impedance. By this approach field changes can be produced within the switch on time scales on the order of 100 ps.

a. Theoretical Design

The functional design of the three-electrode switch may be described with reference to Figure 2. Static potential $-V_o$ is placed upon the main electrodes to produce the initial field E_o. An impulsive trigger signal of pulse height V_t is fed to the third electrode through a blocking capacitance C, thereby producing additional fields E_{t1} and E_{t2} in regions (1) and (2), respectively. Unequal spacings d_1 and d_2 are visualized in these regions.

In operation E_o is some fraction f of the self-breakdown field E_B. The triggering impulse produces total fields E_1 and E_2 which are given by:

$$E_1 = E_{t1} + E_o$$
$$E_2 = -E_{t2} + E_o \qquad (1)$$

It is then assumed that the trigger signal and gap spacings are arranged so that

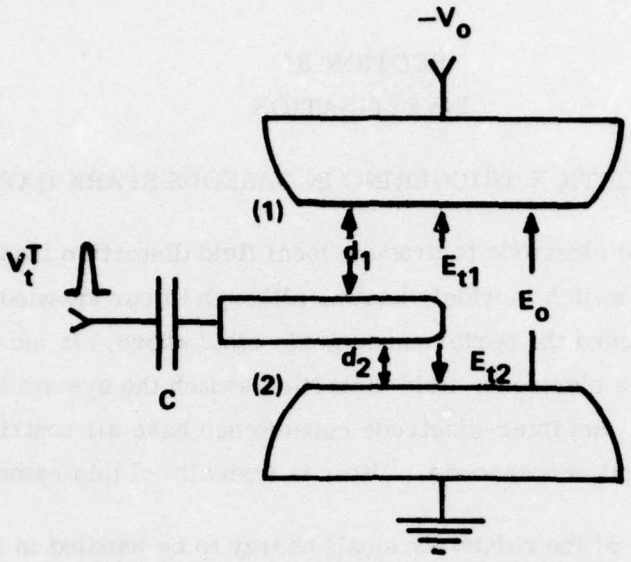

Figure 2. Field Configuration in Three-Electrode Switch

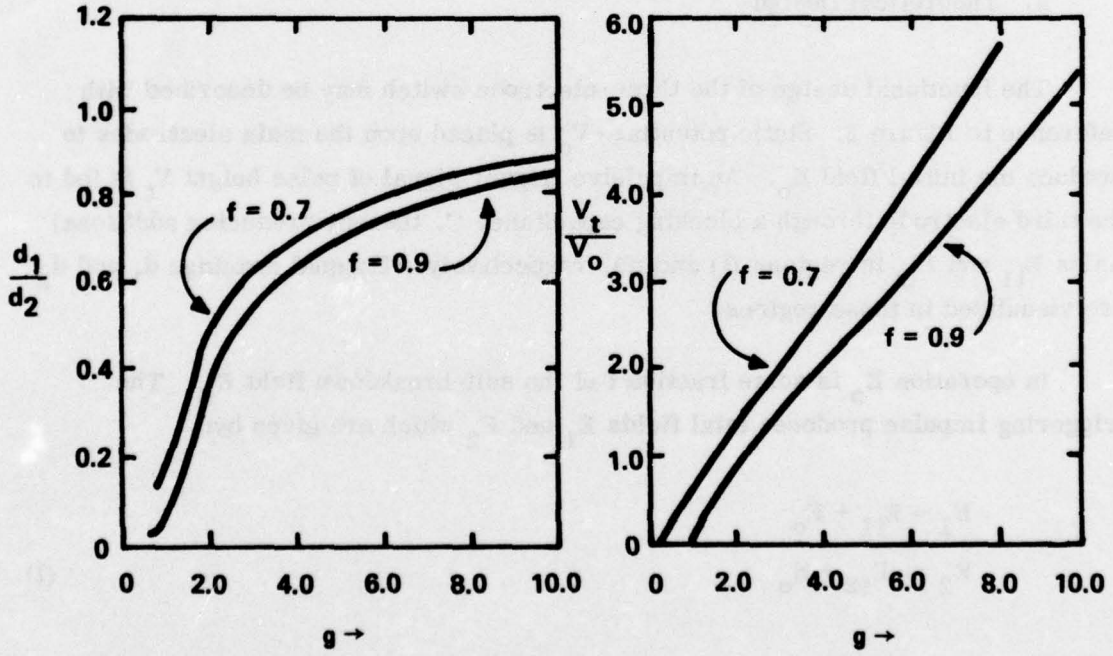

Figure 3. Performance Parameters Field Distortion Switch

$E_1 = E_2 = g\,E_B$; that is, both regions of the divided portion of the switch are placed in a similar overvoltage state where g is the overvoltage ratio.

Substitution in (1) and noting that $V_t = d_1 E_{t1} = d_2 E_{t2}$ leads to relationships between g, f, d_1, d_2, V_t and V_o as follows:

$$\frac{d_2}{d_1} = \frac{g - f}{g + f} \tag{2}$$

$$\frac{V_t}{V_o} = \frac{g^2 - f^2}{2gf} \tag{3}$$

These dimensionless parameters are plotted in Figure 3 against the degree of trigger overvoltage g for two values of f. The curves indicate the critical importance of achieving rapid triggering with a relatively small value of g, say $g < 2$. Otherwise, the trigger pulse height must be greater than the potential being switched, a situation which would eventually cause the method to be an impractical one.

The determination of the required overvoltage ratio and other design parameters follow from a particular model of the switch operation. We assume that the lag time in closure of the spark gap consists of two distinct components: the statistical lag time τ_s and the formative lag τ_f. Thus,

$$\tau = \tau_s + \tau_f \tag{4}$$

It is further assumed, as we have done previously,[1] that τ_s is determined solely by field emission to form a critical charge density of initial electrons. Based upon empirical data,[8] the statistical lag time can be expressed by:

$$\tau_s = 7 \times 10^3\, E^{-2} \exp 870/E \tag{5}$$

where τ_s is in nanoseconds and E is in kilovolts/cm. In this estimate of the statistical lag component, the effect of finite risetime of the impressed field E has been disregarded. Based on this model, the statistical lag time, which we have equated to

jitter, has the dependence illustrated in Figure 4. The values of E_1 and E_2 must then be approximately 700 kV/cm to achieve the objective 50 ps jitter. Of course, any finite risetime of the triggering pulse will contribute to jitter. Thus, in general, even larger values of the initiating field will be required.

The formative time is a measure of the rapidity with which an arc will form following the statistical events responsible for τ_s. Controlled by collisional processes in the gas, the formative time may be expressed most simply by:

$$\tau_s = \frac{\ell n(n_b/n_o)}{\upsilon_i - \upsilon_a} \tag{6}$$

where n_b/n_o is the ratio of the electron density at breakdown to the initial density, and υ_i and υ_a are the ionization and attachment frequencies, respectively. The breakdown process then depends upon the electric field, the gas pressure and, of course, the species. Formative time processes taking place on a nanosecond scale have been measured for several gases.[14] The experimental data for air are plotted in Figure 4 as a function of pressure at the field strength required for jitter near 50 ps. The formative time is a measure of delay and is also related to the risetime. Figure 4 suggests that the entire pressure range illustrated would be suitable from this viewpoint for most Hertzian devices.

Determination of the overvoltage ratio as a function of pressure points strongly toward the use of operating pressure near 10^4 Torr (~ 200 lb/in.^{2}). For air, the self breakdown field is approximately $E_B = 35P$. Thus, in applying triggering fields of 700 kV, the overvoltage ratio is given by:

$$g = \frac{2 \times 10^4}{P} \tag{7}$$

The desirable small values of g can therefore be obtained only at gas pressures near 10^4 Torr or above.

Typical design parameters of an impulsively triggered, field distortion switch may be tabulated as follows:

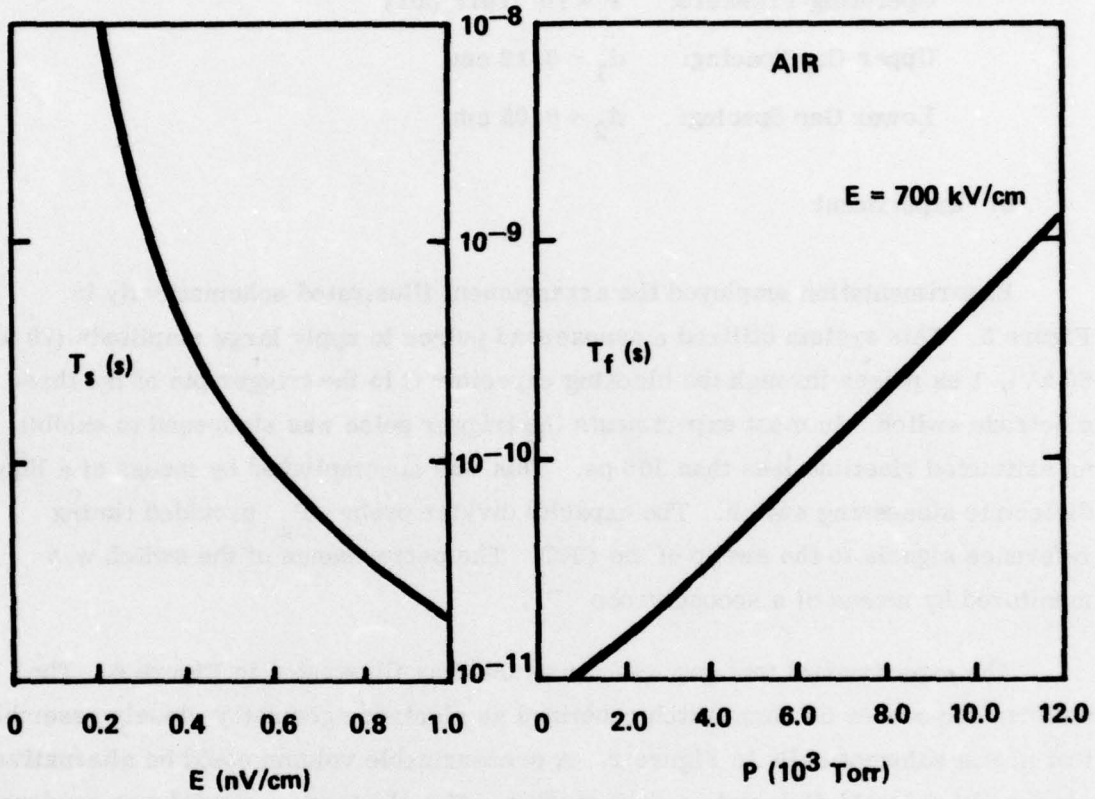

Figure 4. Statistical and Formative Time Dependencies

Operating Voltage: $V_o = 60$ kV

Undervoltage Ratio: $f = 0.8$

Overvoltage Ratio: $g = 2.0$

Trigger Pulse Height: $V_t = 63$ kV

Operating Pressure: $P = 10^4$ Torr (air)

Upper Gap Spacing: $d_1 = 0.12$ cm

Lower Gap Spacing: $d_2 = 0.05$ cm

b. Experiment

Experimentation employed the arrangement illustrated schematically in Figure 5. This system utilized a nanosecond pulser to apply large amplitude (10 to 50 kV), 1 ns pulses through the blocking capacitor C to the trigger pin of the three electrode switch. In most experiments the trigger pulse was steepened to exhibit an estimated risetime less than 100 ps. This was accomplished by means of a liquid dielectric steepening switch. The capacity divider probe P_2 provided timing reference signals to the sweep of the CRO. The performance of the switch was monitored by means of a second probe P_1.

The experimental test gap was constructed as illustrated in Figure 6. The uniform impedance 50 ohm switch contained an electrode geometry closely resembling that shown schematically in Figure 2. A pressurizable volumn could be alternatively employed for liquid dielectric switch studies. The electrode material was hardened steel, a material which we have found to be similar electrically to tungsten or tungsten-copper, but one which suffers less mechanical damage under sparking conditions. The latter is of paramount importance in liquid switches where wear processes seem to be more severe than those observed in gases.

Typical test results are shown in the oscilloscope photo in Figure 7. These waveforms, the output of capacitive divider P_1, show the initial spike at t_t, which results when the stray capacitance of the trigger pin is discharged through breakdown. The main pulse launched at time t_m exhibits an apparent delay $t_m - t_t$. The oscilloscope was triggered by the method illustrated in Figure 7, and two superimposed traces in each case illustrate little measurable jitter in either t_t or in t_m.

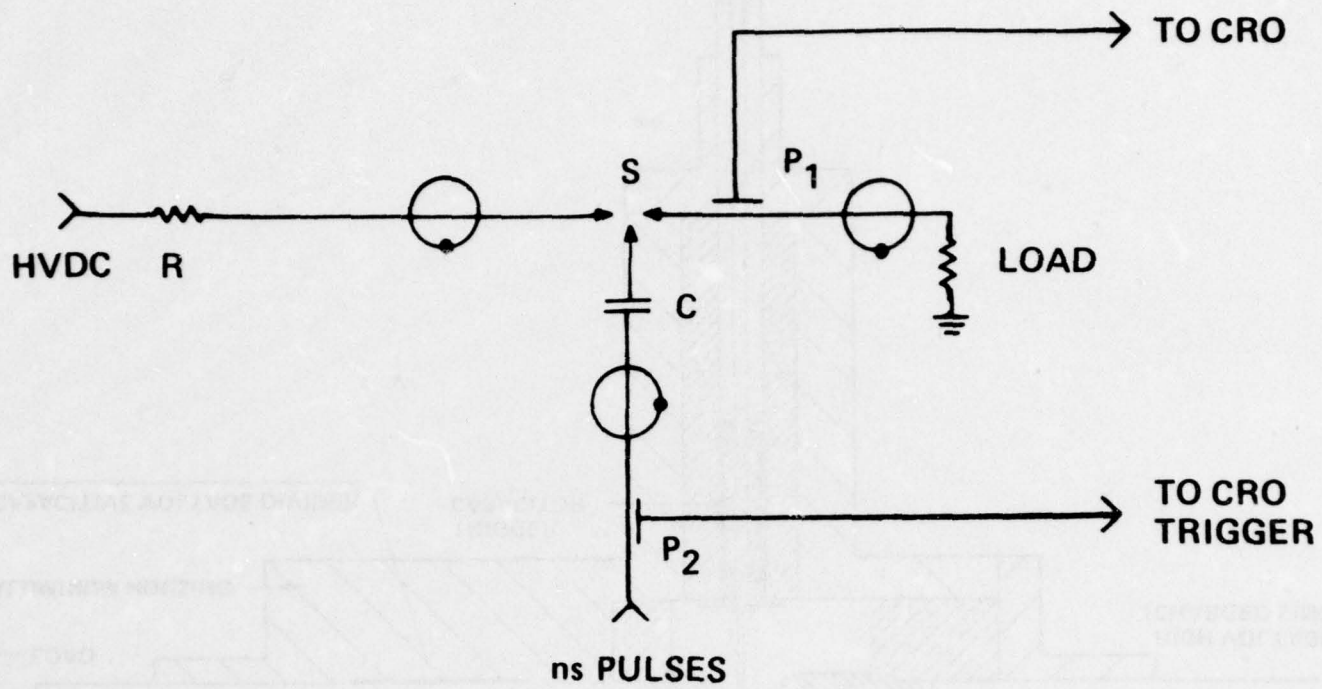

Figure 5. Schematic of Field Distortion Trigger Experiment

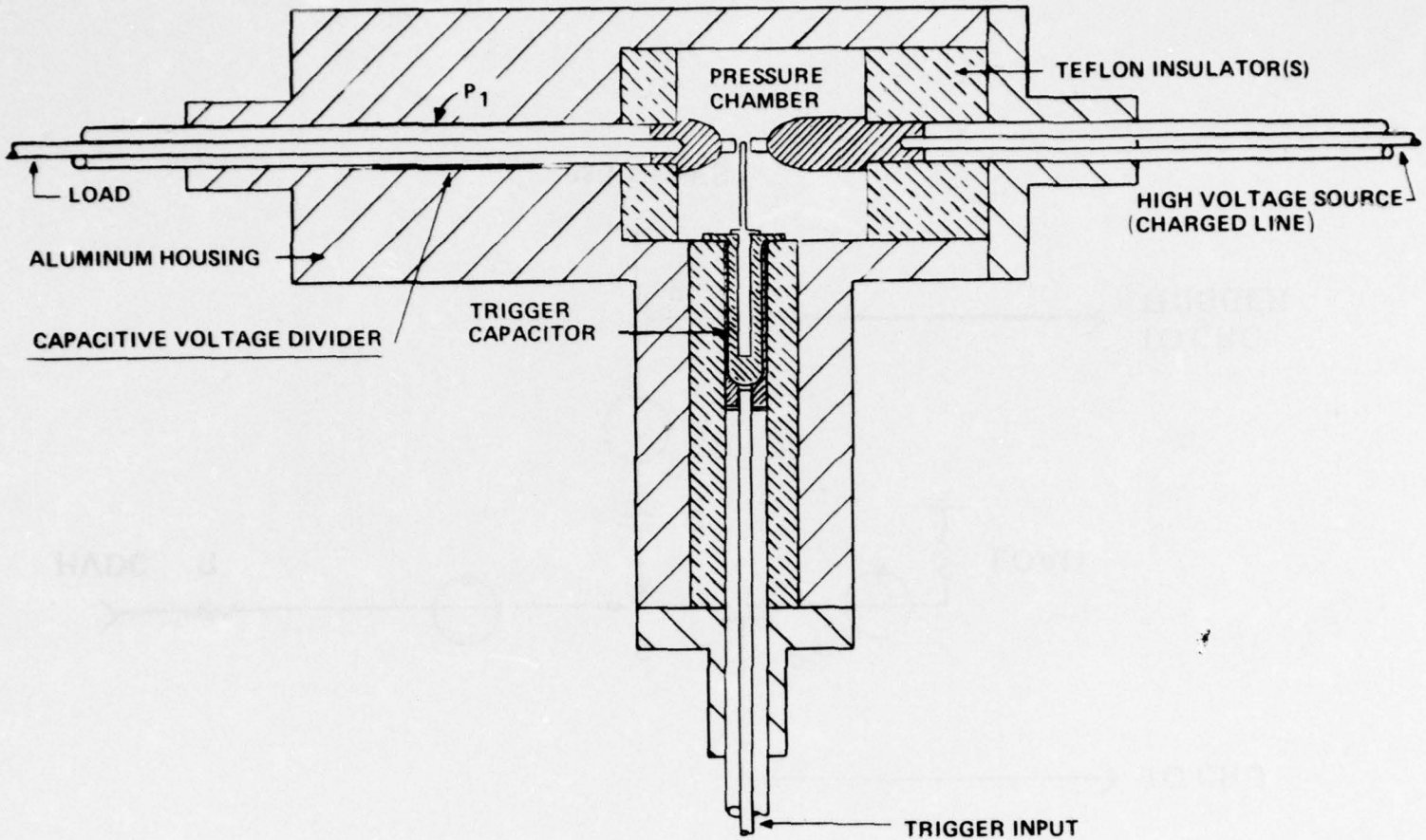

Figure 6. Field Distortion Triggered Spark Gap

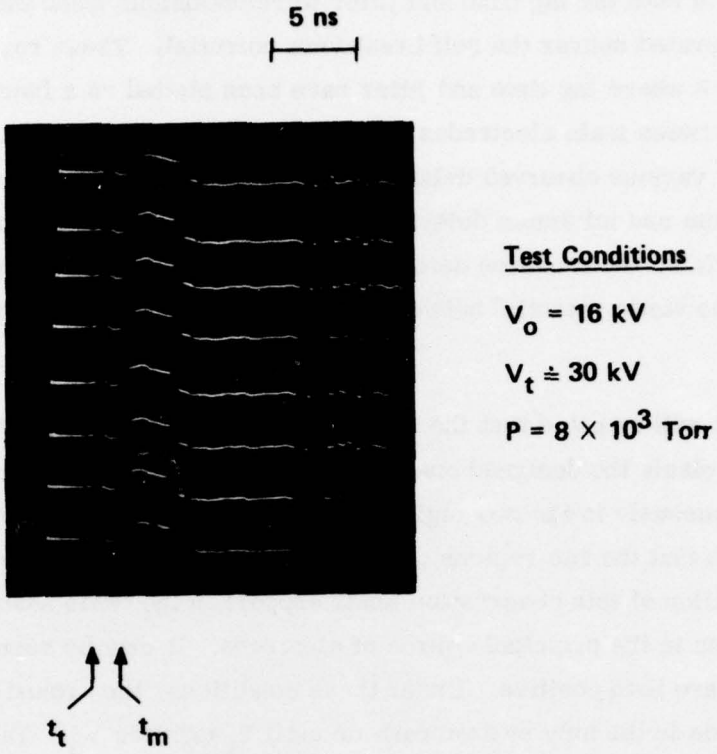

Figure 7. Typical Field Distortion Switch Performance

Detailed measurements of the time lag and jitter under the conditions illustrated in Figure 7 yield an average lag time of 3.4 ns and a jitter of 0.15 ns. Yet smaller values of both the lag time and jitter were obtainable when the same gap arrangement was operated nearer the self breakdown potential. These results are summarized in Figure 8 where lag time and jitter have been plotted as a function of V_o, the potential drop between main electrodes. V_o/V_B is then a measure of the degree of undervoltage for various observed delays and jitter values. The two curves, illustrating maximum and minimum delay, indicate the extreme values noted in a series of lag time trials. Both curves demonstrate that the jitter is substantially sub-nanosecond when the static potential between main electrodes exceeds about 70% of self-breakdown.

It will be noted that the switching function exhibited in the above experiments is not precisely the designed one. Thus, it appears that closure does not take place simultaneously in the two regions of the gap space (see Figure 2). Instead the data indicate that the two regions of the gap undergo breakdown sequentially. The explanation of this observation lends support to the basic assumption that field emission is the principal source of electrons. It may be seen in Figure 7 that V_o and V_t are both positive. Under these conditions, the ground referenced output electrode is the only system cathode until V_t exceeds V_o. This tends to produce an initiating breakdown event in this portion of the switch. Subsequently, the trigger electrode falls to ground potential so that an overvoltage condition is produced in the second gap space leading to a delayed closure of the switch.

Switch function, in which both halves of the switch were simultaneously closed, was achieved by choosing polarities as in the model of Figure 2. A narrow, impulsive triggering pulse was generated which was less than 1 ns in width (FWHM) with risetime estimated to be less than 100 ps. A photo of this waveform, as displayed on a 1 GHz oscilloscope, is shown in Figure 9(a). The triggered waveform, as observed with the apparatus shown in Figures 5 and 6, is illustrated in Figure 9(b). In this case approximately 100 sweeps are superimposed. The positive impulse is due to interelectrode signal coupling. It may be seen that the delays noted previously are no longer present. Jitter is estimated to be near 100 ps or less, relative to the triggering impulse. It is noteworthy that one or more missed closures are in evidence, a factor of significance in large arrays (see Section 2b).

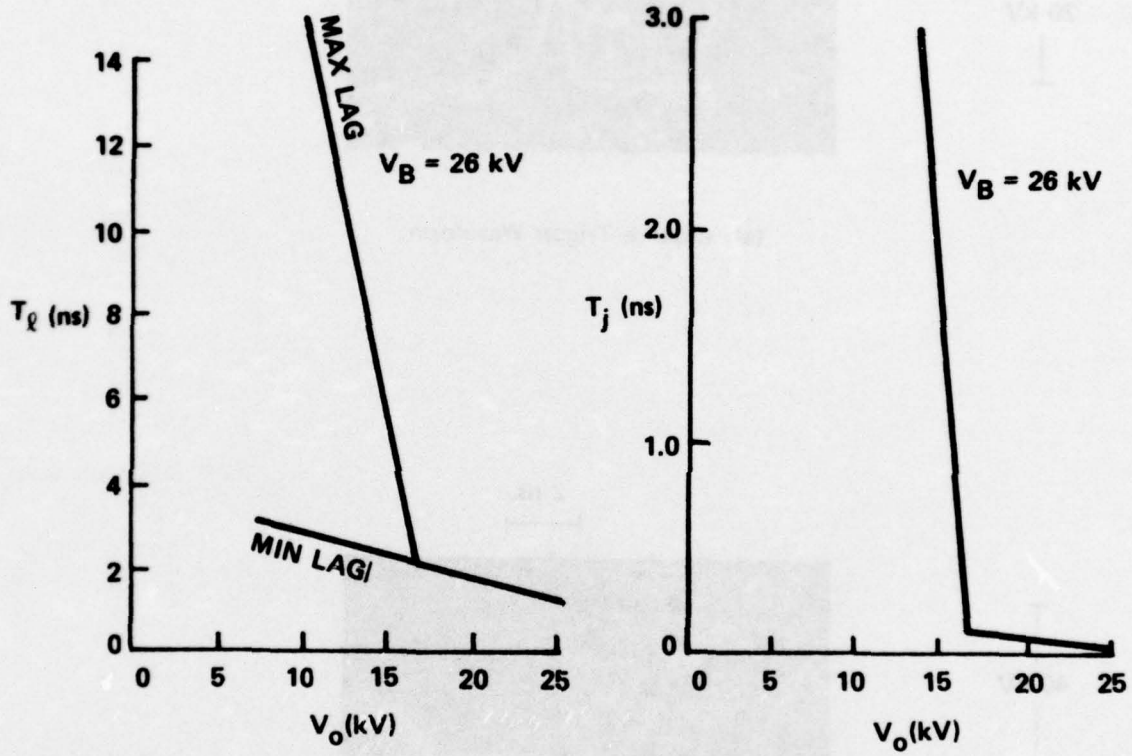

Figure 8. Triggering Characteristics of Field Distortion Switch
Left, lag time; Right, jitter.

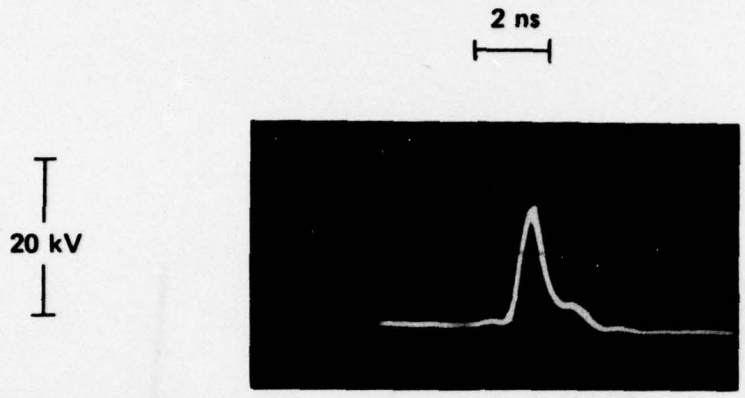

(a) Impulse Trigger Waveform

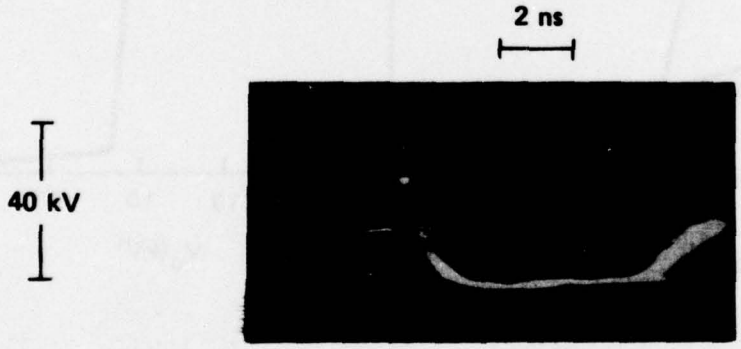

(b) Impulse Triggered Square Wave

Figure 9. Impulse Field Distortion Waveforms

Subsequent experimentation was performed with two identical switches of the field distortion type. These were greatly simplified versions of the three electrode switch shown in Figure 6. The impulsive triggering of these switches, while similar in behavior to that illustrated in Figure 9, produced a larger percentage of missed closures, probably due to the necessary division of trigger signals. This division and its attendant degradation of switch performance is one which becomes more serious and more difficult to overcome as the array increases. Therefore, we have sought alternative approaches in this investigation.

2. LIQUID ELECTRONIC SWITCHING

a. Liquid Breakdown

In a research effort* predating this investigation, some positive indications were established that electron multiplication (Townsend) processes may exist in certain liquids, particularly aprotic liquids.[11, 15] Pursuing the rationale that energetic electron processes are impeded by C-H bonds whose vibrational excitation constitutes an energy sink for electrons,[16] we undertook an effort to find impact ionization phenomena in simple liquids lacking such bonds. A particularly striking demonstration of the positive findings of this work is illustrated in molten sulfur (Figure 10) in which 50 mJ spark discharges were produced in the liquid without phase change at repetition rates of the order of 10^2 Hz. Liquid sulfur has subsequently been the subject of a more exhaustive study of high field transport and photoconduction properties. The current-voltage characteristics (Figure 11), seem to result from bulk effects and the particular dependence illustrated suggests a tunneling process wherein trapped electrons (and holes) are induced to tunnel from localized states into a quasi-conduction band. Carriers of both species then gain energy in the field and may eventually suffer energetic collisions leading to multiplication.

In the early portion of the present investigation an attempt was made to exploit these new found liquid properties and to find means for the rapid initiation of break-

*Partially supported by the Office of Naval Research under Contract N00014-74-C-0215.

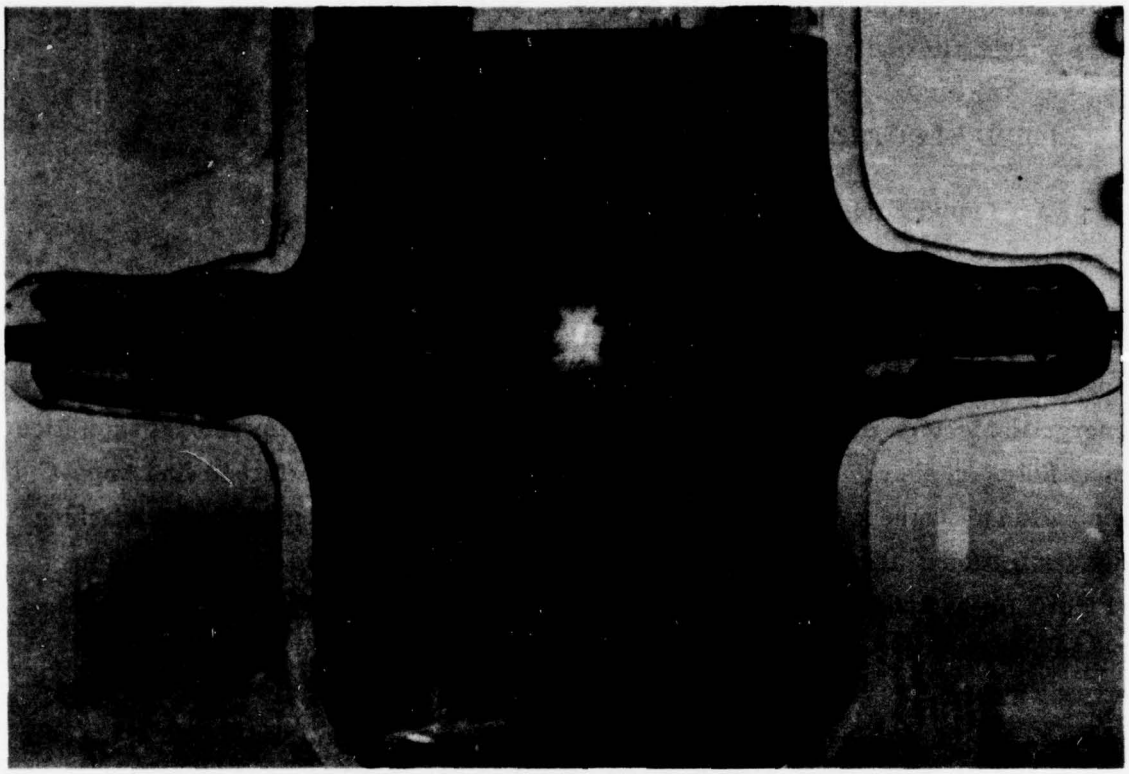

Figure 10. Repetitive Spark Breakdown in Liquid Sulfur

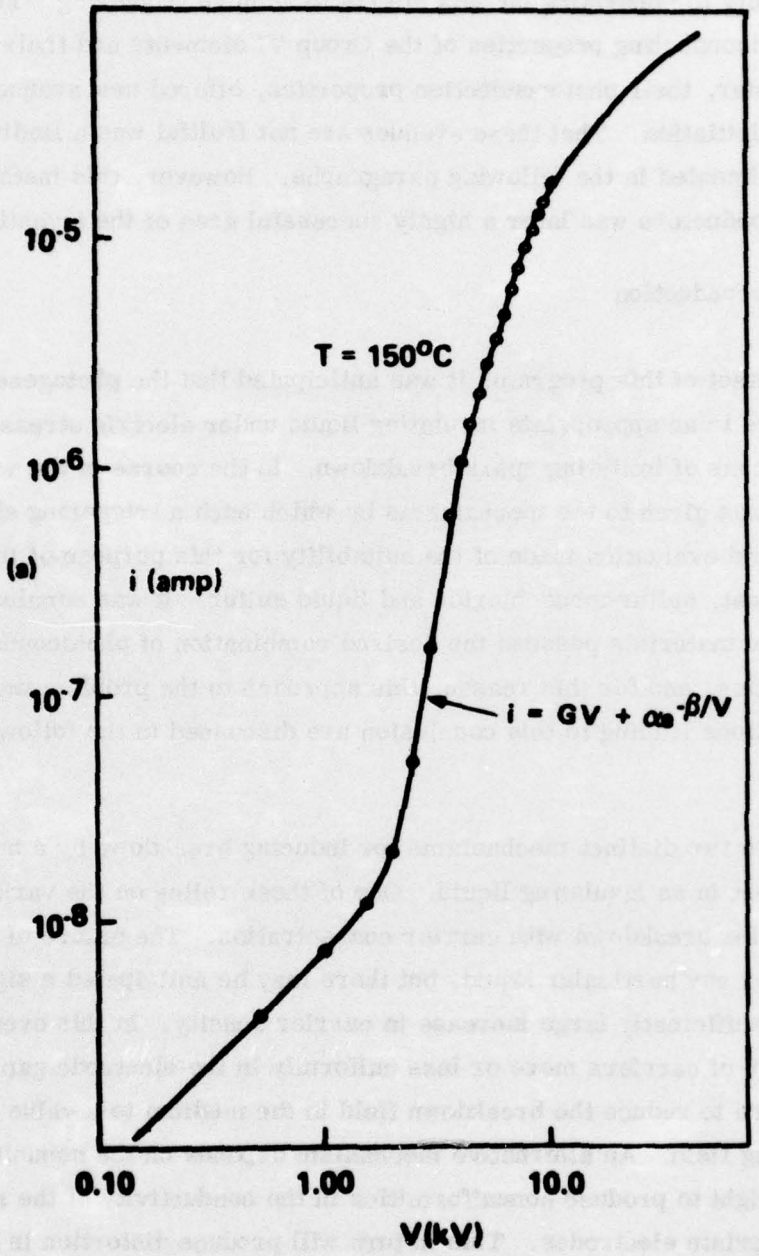

Figure 11. High Field Conduction in Liquid Sulfur

down. One of the important distinctions between liquids and gaseous dielectrics lies in the opportunity for operating on bulk effects to achieve triggering. For example, the known semiconducting properties of the Group VI elements and their compounds and, in particular, their photoconduction properties, offered new avenues for optical switch initiation. That these avenues are not fruitful was a finding in this program as delineated in the following paragraphs. However, this method of triggering in solid semiconductors was later a highly successful area of the investigation.

b. Photoconduction

At the outset of this program, it was anticipated that the photogeneration of charge carriers in an appropriate insulating liquid under electric stress would be an effective means of initiating spark breakdown. In the course of the work, detailed consideration was given to the mechanisms by which such a triggering effect might be obtainable and evaluation made of the suitability for this purpose of the liquids of principal interest, sulfur monochloride and liquid sulfur. It was concluded that neither of these materials possess the desired combination of photoconductive and optical properties, and for this reason, this approach to the problem was abandoned. The considerations leading to this conclusion are discussed in the following paragraphs.

There are two distinct mechanisms for inducing breakdown by a bulk photoconductive effect in an insulating liquid. One of these relies on the variation of the field required for breakdown with carrier concentration. The nature of this variation is not known for any particular liquid, but there may be anticipated a significant effect given a sufficiently large increase in carrier density. In this event, the photogeneration of carriers more or less uniformly in the electrode gap of a discharge cell would serve to reduce the breakdown field in the medium to a value below that of the pre-existing field. An alternative mechanism depends on the nonuniform absorption of light to produce nonuniformities in the conductivity of the medium between appropriate electrodes. This in turn will produce distortion in the electric field, the field being increased in regions of least light absorption. If the original field was slightly below the breakdown of the medium, this increase should serve to trigger the discharge.

Whichever of these mechanisms is operative, the general requirements on the material are similar: it should show a good photoresponse at wavelengths where it is a moderately good absorber, i.e., where the radiation will penetrate into an appreciable fraction of the volume between the electrodes. In effect this means that the absorption coefficient of radiation to which the medium shows high photosensitivity should be of the order of the reciprocal of the gap dimensions.

Experiments on the photoconductive properties of the liquids of interest were carried out in the cell shown schematically in Figure 12. A desirable feature of this cell is that the exciting radiation is introduced through the transparent platinum coating which forms one electrode. Therefore, all absorption occurs in the high field region regardless of the magnitude of the absorption coefficient. In most cases the source was a 100 W high pressure mercury arc lamp which provided radiation from about 600 to 280 nm.

So far as is known, no earlier reports exist on the photoconductive properties of sulfur monochloride. The results of the present tests were essentially negative in that no response was observed that could be interpreted as true photoconduction. A small modulation of the cell current by light (about 0.1%) was observed for one direction of applied field but not the other. This response was the reverse of the usual photoeffect in that the effect of the light was to reduce the current, and was probably due to an interaction at one of the electrodes. Thus, sulfur monochloride is at best a very poor photoconductor and not a promising candidate for the desired application.

The case of sulfur is somewhat different. Data are available on its photoconductive and optical properties in the liquid states indicating that it is at least a moderately sensitive photoconductor. Ghosh and Spear[17] have reported the spectral dependence of its photoconductive quantum efficiency. Their results are plotted in curve 1 of Figure 13. While detailed spectral measurements were not made as a part of this program, observations in the cell of Figure 12 were compatible with these results. They showed a substantial photoconductive effect in liquid sulfur due to ultraviolet radiation but essentially no response to visible radiation. Also shown in Figure 13 is the absorption coefficient of liquid sulfur as reported by Meyer, Oommen, and Jensen.[18] A large difference in wavelength between the absorption edge and the onset of

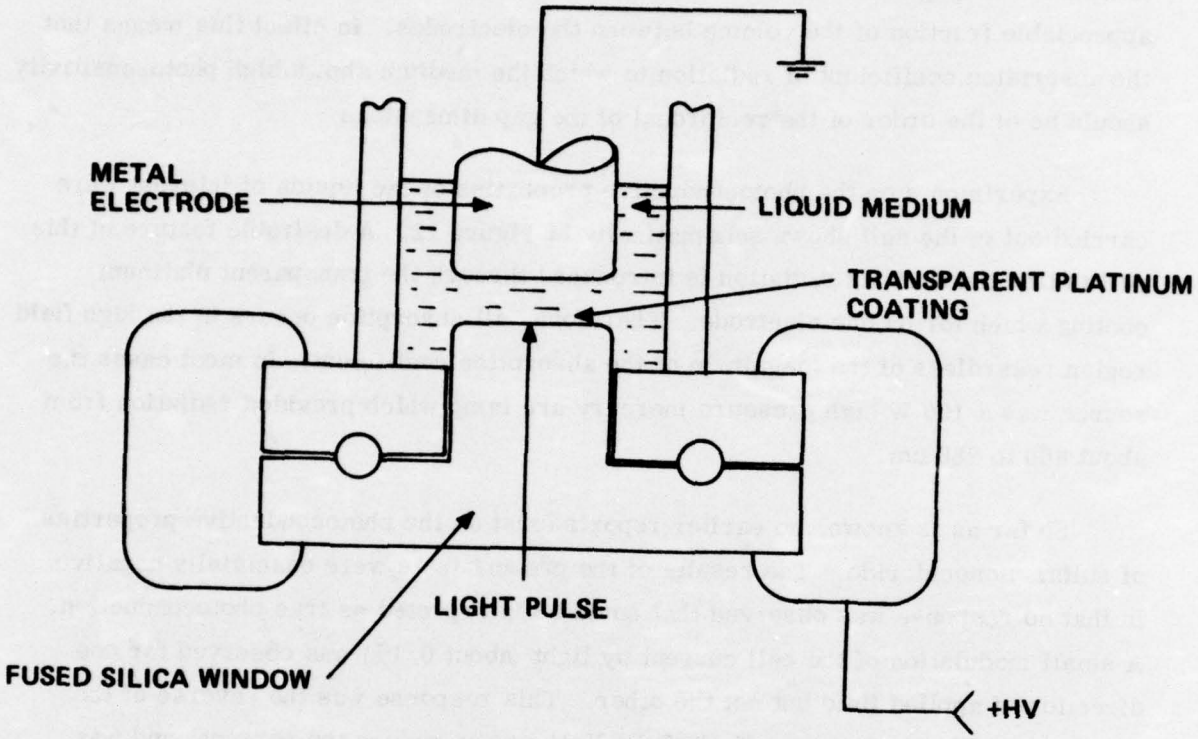

Figure 12. Experimental Photoconductivity Cell

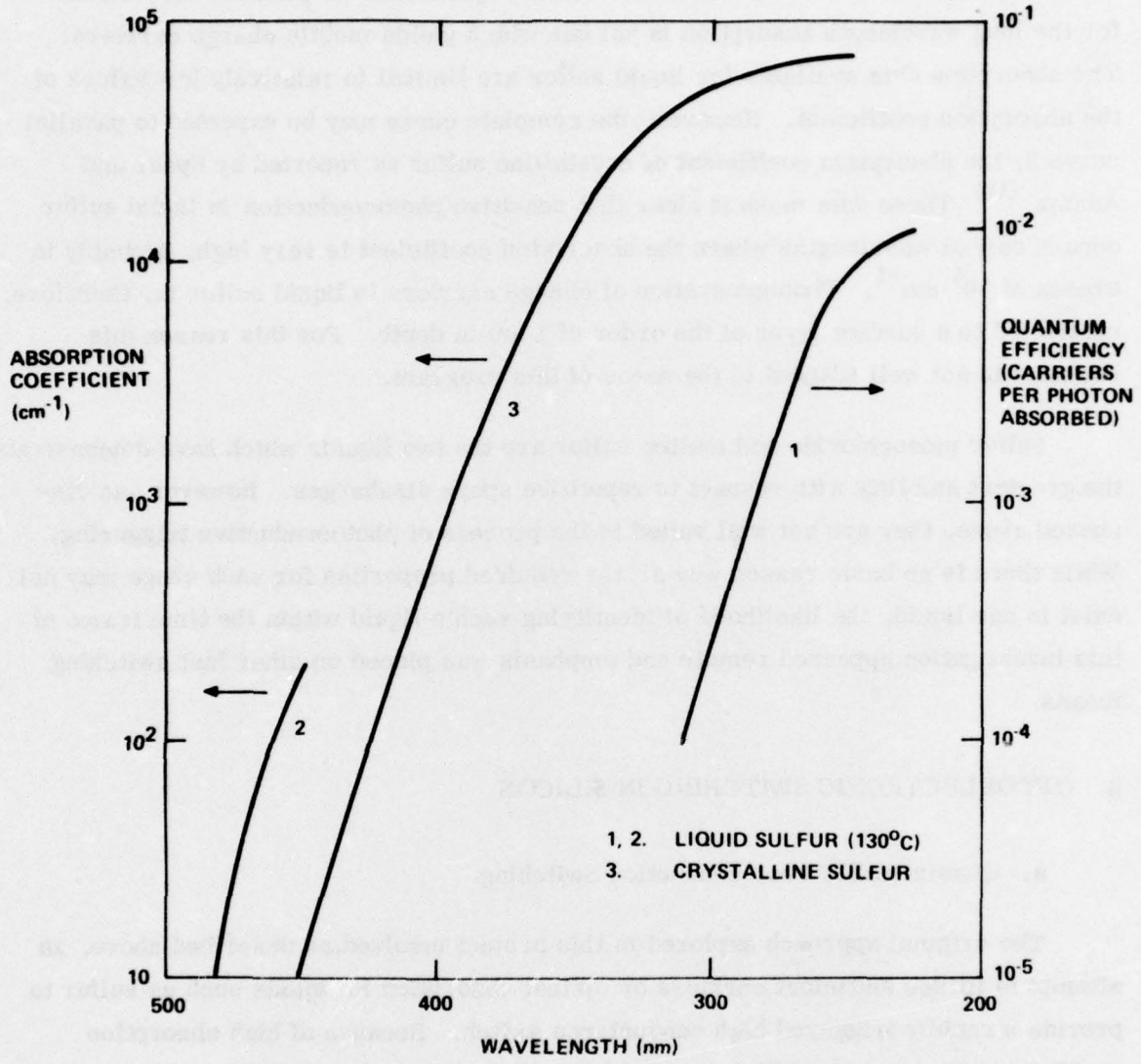

Figure 13. Photoconduction and Optical Absorption in Sulfur

efficient photoconduction is in evidence. This implies that the process responsible for the long wavelength absorption is not one which yields mobile charge carriers. The absorption data available for liquid sulfur are limited to relatively low values of the absorption coefficient. However, the complete curve may be expected to parallel curve 3, the absorption coefficient of crystalline sulfur as reported by Spear and Adams.[19] These data make it clear that sensitive photoconduction in liquid sulfur occurs only at wavelengths where the absorption coefficient is very high, probably in excess of 10^4 cm^{-1}. Photogeneration of charge carriers in liquid sulfur is, therefore, restricted to a surface layer of the order of 1 μm in depth. For this reason this material is not well adapted to the needs of this program.

Sulfur monochloride and molten sulfur are the two liquids which have demonstrated the greatest stability with respect to repetitive spark discharges. However, as discussed above, they are not well suited to the process of photoconductive triggering. While there is no basic reason why all the required properties for such usage may not exist in one liquid, the likelihood of identifying such a liquid within the time frame of this investigation appeared remote and emphasis was placed on other fast switching means.

3. OPTOELECTRONIC SWITCHING IN SILICON

a. Quasimetallic Photoconduction Switching

The original approach explored in this project involved, as described above, an attempt to induce sufficient carriers by optical absorption in liquids such as sulfur to provide a rapidly triggered high conductance switch. Because of high absorption coefficient, low quantum efficiency and large dielectric relaxation time, this approach has been shown to be unfeasible. Coincidentally, research at Bell Laboratories was reported[12] at about this time in which successful attempts were made to accomplish this same switching function in silicon. It has been shown that a laser delivering microjoule pulses can produce quasimetallic photoconduction in silicon with a corresponding change in conductance from 10^{-4} $(ohm\text{-}cm)^{-1}$ to 10^{3} $(ohm\text{-}cm)^{-1}$. The switching speed is limited only by the optical pulse since the dielectric relaxation time is less than 1 ps. Electrical signals as large as 100 V (and probably much

higher) can be switched. Auston demonstrated pulse widths of 15 ps at power levels of the order of 100 W. Zucker, et al[13] report nanosecond risetime switching with multimegawatt peak power in light-activated multilayer silicon devices.

In the present investigation, we undertook a set of experiments to demonstrate the feasibility of this method of switching in multiswitch arrays making up the Frozen Wave Generator. Working with high resistivity silicon and a gas laser, we were able to achieve quasimetallic conduction and virtually exact synchronism of multiple switches in this generator. The significance in the results, in conjunction with those of Auston and Zucker, lies in the possibility of generating megawatt pulses in the higher microwave bands by solid semiconducting devices. This performance is far beyond that of known junction devices. In view of the phase stability of the switches composing an array, even more power could be achieved by coherent addition of multiple sources. Ultimately, the power might exceed the reasonable expectations of spark gap devices.

b. Single Channel Switch

Initial experimentation was performed using an 0.020 in. wafer of 5×10^4 ohm-cm silicon upon which was placed a metallized microstrip transmission line as shown in Figure 14. A gap in the microstrip line, ranging between 0.005 and 0.025 in. for various experiments, permitted the light pulse from the laser to penetrate the silicon surface. Thus, a conducting sheet was formed in the gap region having the real dimensions of the illuminated gap and a depth equal, approximately, to the reciprocal of the absorption coefficient. In the devices considered by Auston, a mode-locked Nd glass laser was used in conjunction with a KDP crystal frequency doubler to produce two timed optical pulses with wavelengths of 0.53 μm and 1.06 μm. The shorter wavelength pulse caused the switch to conduct as just described, while the delayed 1.06 μm pulse was used to penetrate the silicon crystal shorting the microstrip line. In our experiments aimed at Frozen Wave Generation, a different approach was taken in which the pulse is shaped by the device (e.g. Figure 1), while the switch is required only to turn on. Thus, dc leakage currents could be reduced in our experiments by means of the insulating Mylar layer depicted in Figure 14(a).

The switch circuit for initial testing is shown in Figure 14(b). A coaxial PFN was used to form a rectangular pulse upon activation of the switch. Experiments

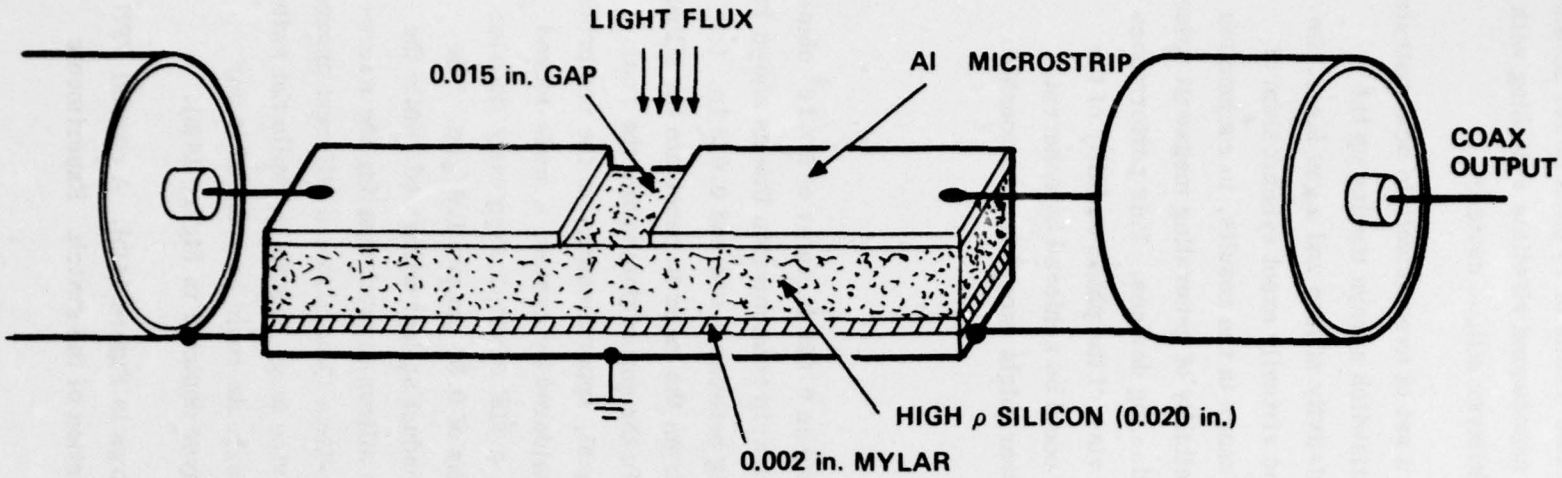

(a) Construction of Optoelectronic Switch

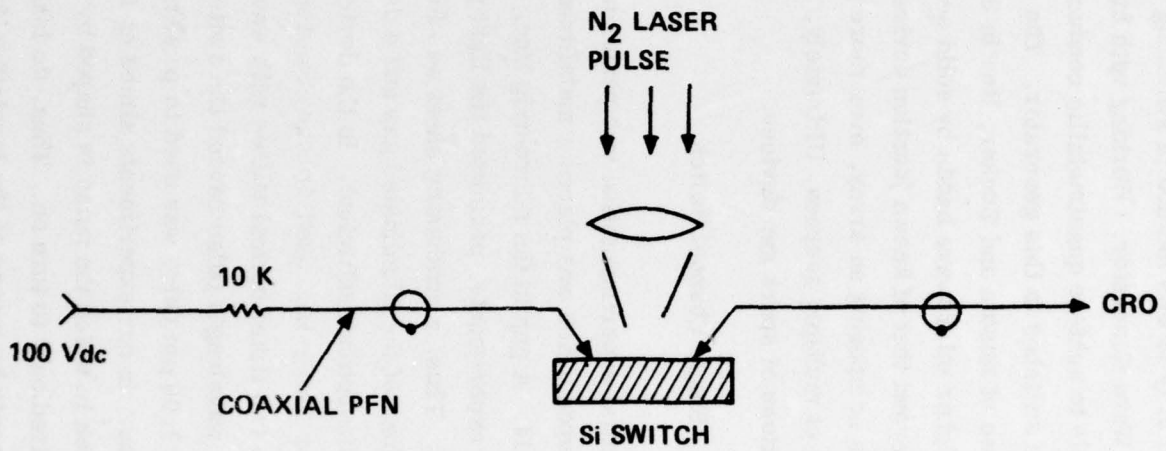

(b) Single Switch Circuit

Figure 14. Single Switch Construction and Test Circuit

were normally performed in the 50 to 100 V range. Higher potentials, perhaps as high as 10^3 V, could have been used if a final dielectric coating of the gap region had been used.

The feasibility experiments were performed with an AVCO Pulsed Gas Laser (Model C950) which produces 10 ns, 1 mJ pulses at 0.34 μm with a typical repetition rate of 10 Hz. This laser was not ideally suited to the demonstrations of quasimetallic photoconduction as may be seen with reference to Figure 15, which is a plot of the room temperature optical absorption coefficient in silicon.[20] The N_2 laser produces a UV pulse where the absorption coefficient is near 10^6 cm^{-1} and where there is, accordingly, very shallow penetration of the silicon. Assuming an illuminated conductivity in Si of 10^{-3} ohm^{-1}, the switch in Figure 14 (a) was expected to exhibit a resistance on the order of 10^2 ohms when closed. The use of 0.53 μm pulses to close the switch would have been preferred in this regard in that the penetration depth and, therefore, switch conductance would have been about 10^2 times greater. Figure 15 also illustrates the relatively large penetration at 1.06 μm which Auston employed for terminating the pulse. The risetime of the N_2 laser was about 2 ns, a value which did not permit the demonstration to be performed at the higher microwave frequencies. These deficiencies were offset to a large degree in our experiments by the relative convenience of the laser and the ability to observe the switching phenomena in real time.

Typical switched pulses are shown in Figure 16. The upper trace was obtained using a 12 ft coaxial cable PFN to generate a 36 ns pulse. An excellent retangular pulse was achieved. The observed risetime, about 3 ns, closely tracked the rise-time of the integrated light pulse. The carriers, produced by photoeffect, persist after the light pulse for a time determined by the shorter of the recombination time or the drift time in the field. The experiment, illustrated in Figure 14(b), was performed to determine this characteristic time. A 100 ft line was used to generate a 300 ns pulse. The observed droop in the launched pulse shape shown in Figure 16(b) is due to the loss of carriers with a characteristic time, in this case of about 200 ns. Various experiments indicated that this decay rate corresponds to the rate at which carriers are swept from the illuminated region of the switch. This relatively slow loss of carriers presents little limitation of the technique when applied to Hertzian arrays, since the latter devices require switch closures which persist for only a few nanoseconds.

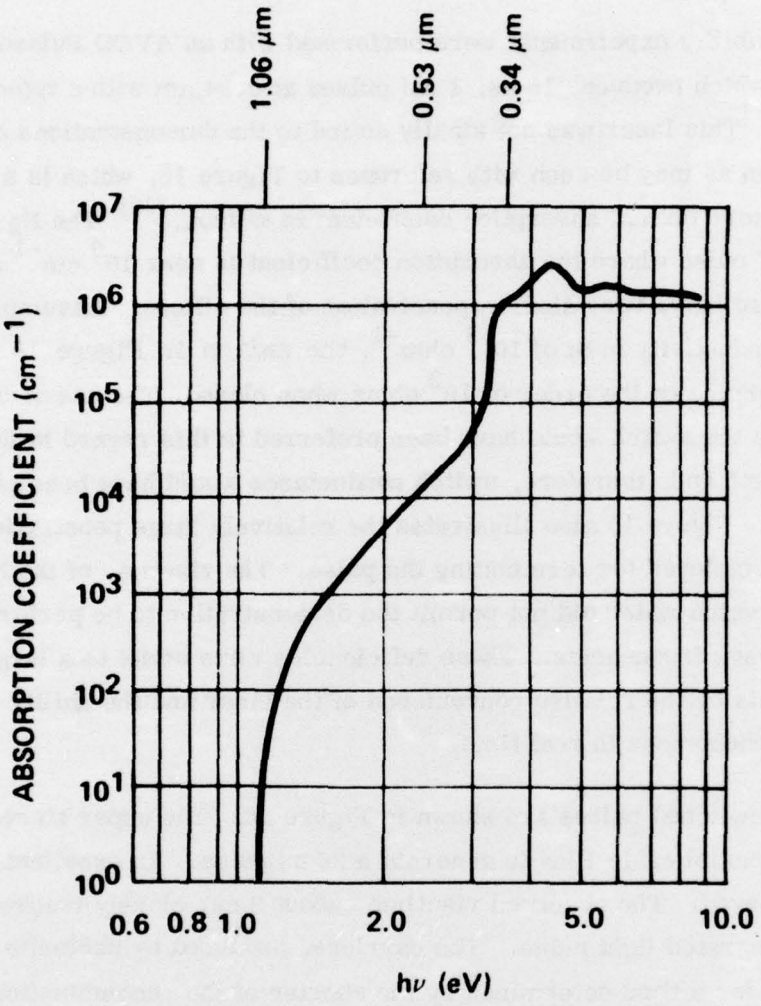

Figure 15. Measured Absorption Coefficient Near Absorption Edge in Si (after SZE, Ref.)

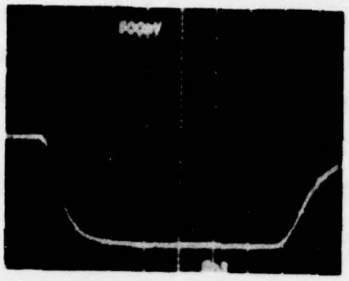

a. 36 ns PULSE

5 ns/lg DIV

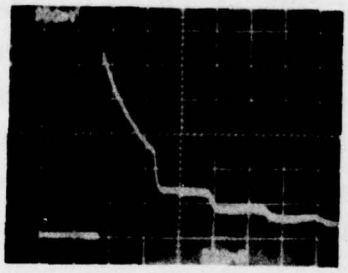

b. 300 ns PULSE

200 ns/lg DIV

Figure 16. Pulse Launched by Single Channel Optoelectronic Switch

c. Optoelectronic Switch Array Experiments

The general success of the single switch experiment led progressively to small arrays of similar switches with provision for variation in the pulse forming circuitry. An array of five elements was arranged in the pattern shown in Figure 17. The five 50-ohm microstrip lines were laid out on a 2 cm diameter disc which was subsequently sliced as indicated and mounted in a microstrip holder. The latter contained microstrip - coax BNC adaptors for each line, making for considerable flexibility in the traveling wave circuitry.

The laser light was focussed into a slit pattern (0.1 × 2 cm) which equally illuminated the switches of the array. The laser delivered an estimated 10^{-6} J to each switch element. Approximately 2×10^{-7} J was then deposited during the first 2-3 ns of the pulse.

The synchronization of two channels was evaluated using two elements of the array shown in Figure 17 with the circuit shown in Figure 18(a). This circuit should produce a negative pulse launched by switch 1 followed, after a total delay of 8 ns, by a similar positive pulse whose leading edge results from the closure of switch 2. If these times of appearance are t_1 and t_2, respectively, the jitter is observed as the variation in $t_2 - t_1$. The waveform illustrated in Figure 18(b) is a superposition of 10 sweeps triggered internally by the first pulse. The jitter is not observable at this sweep rate and must be less than the apparent time interval occupied by the trace-width, in this case, less than 100 ps.

Three elements of the array were arranged in the circuit shown in Figure 19(a). In this case a two cycle waveform was expected and was observed as seen in Figure 19(b). The beginning of the second cycle corresponds to closure of switch element 3. Its timing under repetitive operation, relative to the first cycle which triggered the CRO, is shown in Figure 19(c). The apparent jitter, if any, is less than about 50 ps.

Further experiments with this array sought to activate all five array elements simultaneously. This objective was realized, although distortions as seen in the second cycle of Figure 19(b) became more pronounced and detracted from the otherwise graphic demonstration of simultaneity. Such distortion probably arose from the

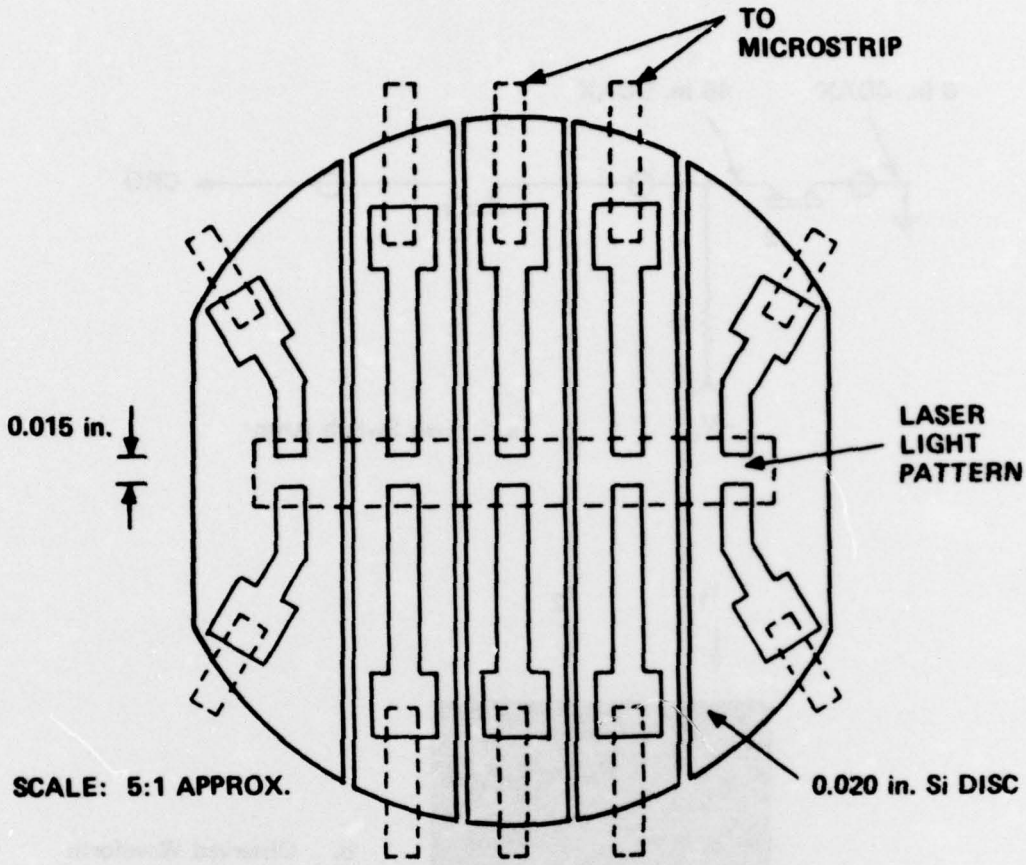

Figure 17. Five Element Optoelectronic Array

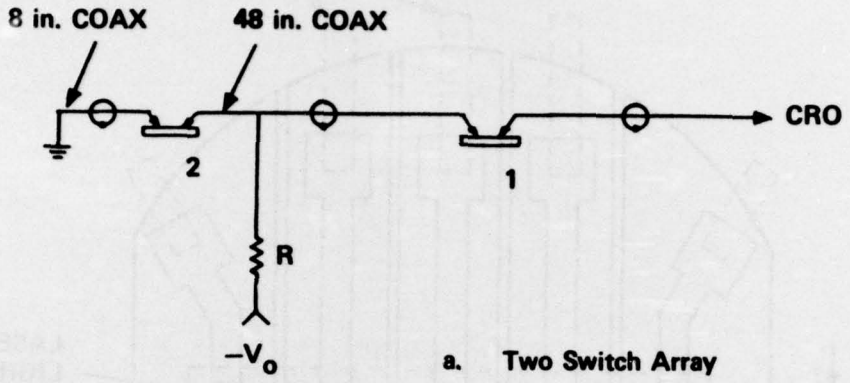

a. Two Switch Array

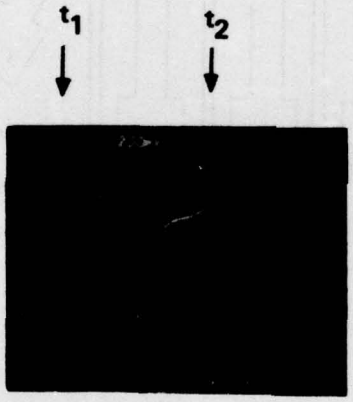

b. Observed Waveform

Figure 18. Two Switch Array and Waveform

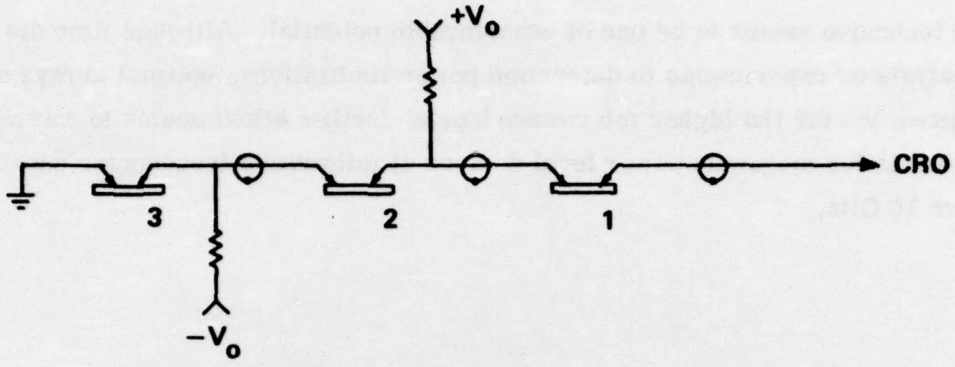

a. Three Switch Circuit

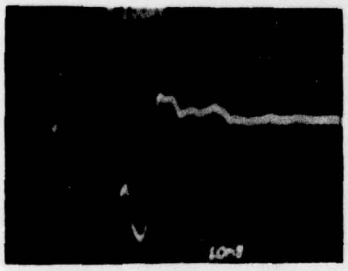

b. Two Cycle Waveform

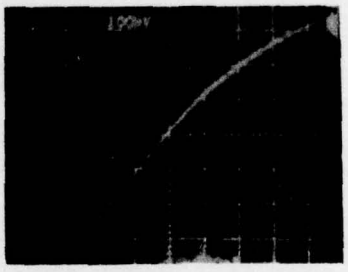

c. Leading Edge of Second Cycle

Figure 19. Three Switch Array and Waveform

failure of the UV laser to produce a truly high conductance state upon switch activation for the reasons cited above.

The technique seems to be one of considerable potential. Although time did not permit analysis or experiments to determine power limitiations, optimal arrays and design approaches for the higher microwave bands, further effort seems to warranted. The potential is for megawatt power level devices at microwave frequencies substantially above 10 GHz.

SECTION IV
SUMMARY AND RECOMMENDATIONS

This investigation has explored mechanisms in all three states of matter which might make possible extremely low jitter switching in Hertzian arrays. Methods involving field distortion triggering in high pressure gases, photoconduction triggering in aprotic liquids and optoelectronic triggering in solid semiconductors have been investigated. The most promising avenue for further research has been identified in the latter area where extremely small jitter and rapid turn-on capabilities are well matched to the timing requirements in Hertzian arrays.

Of the three methods which were investigated in this study, the three electrode, potential divided gap was least innovative. However, success was achieved in extending the control of such gaps to obtain jitter less than 100 ps. This was accomplished by minimizing the interelectrode capacitance and by driving the switch with an impulsive triggering pulse of sub-nanosecond width. The difficulty in the method, as applied to Hertzian arrays, lies in the statistics of jitter as influenced by the extremely short, high amplitude trigger pulse. The probability of missed closures, while not large for the individual switch, looms as a critical quantity in large series arrays such as those involved in the Frozen Wave Generator. The procedures which might be applied to overcoming this fault would appear to be energy inefficient and complex, thus defeating the important simplicity/efficiency features of Hertzian devices.

Switch mechanisms in the liquid state were investigated based upon newly found evidence for repetitive discharges in aprotic liquids involving electron multiplication within the liquid phase. The particular triggering method which was explored involved the photogeneration of carriers in the bulk material. The molecular liquid candidates which were studied failed to exhibit the desired combination of photoconductive and optical absorption properties and the approach was abandoned. However, this switching technique could be a valuable one should the appropriate liquid be found, since liquid media offer certain advantages over both gases and solids in spark switching application. The rapidly expanding research in amorphous and liquid semiconductors may eventually reveal one or more liquids with the appropriate optical and chemical properties.

Recently reported work by others has demonstrated a fast switching mechanism in silicon with a potential for performance in terms of power handling and speed that is far beyond that of semiconducting junction devices. This mechanism involves the formation of a quasimetallic conduction state in silicon by means of a low energy visible light laser pulse. The switching speed is limited only by the laser pulse shape and may be as rapid as 10 ps. By appropriate series-parallel arrays it is possible to handle megawatts of power. A successful effort in the present investigation sought to apply and evaluate this method of switching in a form which might apply to Hertzian arrays. The technique was demonstrated in this context in a small array composing a Frozen Wave Generator.

To date, the simplicity, high peak power capability, and short pulse/wide bandwidth capabilities have been over-riding factors governing the interest in Hertzian devices. However, their renowned poor signal quality has precluded their wider acceptance and use in many applications. Spurious spectral features including harmonics, random frequency modulation and noise are characteristic of virtually all Hertzian devices developed to date. Stabilization of the fast switching function of these generators could remove some or all of these limiting characteristics. The potential of quasimetallic photoconduction switching in solid state devices appears to offer the promise of such stabilization at substantial power levels. It is, therefore, recommended that further effort be applied toward realization of this potential. Principal areas of investigation should look toward optimizing the optical radiation source and its distribution, toward optimal arrangements of switch elements for power handling, and toward the delineation of the relationships between power handling limits and device lifetime. Beyond this, the technology of opto-electronic switching appears to offer important new avenues of development and new use-modes in solid state Hertzian devices which should be pursued.

REFERENCES

1. W. H. McNeill and J. M. Proud, "Microwave Hertzian Generator Investigation," RACD-TR-74-33. AD#777881/4GI.

2. H. Cronson, U. S. Patent No. 3,748,528

3. J. M. Proud, U. S. Patent No. 3,484,619

4. J. M. Proud, et al, RADC-TR-68-254. AD#838898.

5. J. M. Proud and W. H. McNeill, RADC-TR-73-227. AD#767907/9.

6. P. Felsenthal and J. M. Proud, "Nanosecond Switch Development," AFWL-TR-65-119.

7. J. R. Bettis and A. H. Guenther, IEEE J. Quantum Electronics, Vol. QE-6, 483 (1970).

8. J. M. Proud and H. J. Huber, "Picosecond Risetime Switch Study," RADC-TR-67-400. AD#820141.

9. A. H. Sharbaugh, 1972 Annual Report Conference on Electrical Insulation and Dielectric Phenomena (National Academy of Sciences, Washington, D. C., 1973) pp. 427-452.

10. J. A. Kok, Electrical Breakdown of Insulating Liquids, Interscience Publishers, New York (1961).

11. J. M. Proud and J. J. Auborn, Appl. Phys. Lett, 27, 265 (1975).

12. D. H. Auston, Appl. Phys. Lett, 26, 101 (1975).

13. O. S. Zucker, et al, UCRL Preprint No. 77449. Proceedings of the International Topical Conference on Electron Beam Research and Technology - Albuquerque (November 1975).

14. P. Felsenthal and J. M. Proud, "Nanosecond-Pulse Breakdown in Gases," Phys. Rev. 139, A1796 (1965).

15. J. M. Proud and J. J. Auborn, "High Field Conduction and Breakdown in Aprotic Liquids," Conf. Elect. Insul. and Diel-Phen. (1975).

16. T. J. Lewis, J. Electrochem. Soc. 107, 185 (1960).

17. P. K. Ghosh and W. E. Spear, J. Phys. Chem. 1, 1347 (1968).

18. B. Meyer, T. V. Oommen, and D. Jensen, J. Phys. Chem. 75, 912 (1971).

19. W. E. Spear and A. R. Adams, J. Phys. Chem. Solids, 27, 281 (1966).

20. S. M. Sze, Physics of Semiconductor Devices, Wiley-Interscience, New York (1969).